Experimental Demonstration of Energy-Chirp Compensation by a Tunable Dielectric-Based Structure

S. Antipov,[1,3] S. Baturin,[5] C. Jing,[1,3] M. Fedurin,[2] A. Kanareykin,[1,5] C. Swinson,[2] P. Schoessow,[1] W. Gai,[3] and A. Zholents[4]
[1]*Euclid Techlabs LLC, Solon, Ohio 44139, USA*
[2]*Accelerator Test Facility, Brookhaven National Laboratory, Upton, New York 11973, USA*
[3]*High Energy Physics Division, Argonne National Laboratory, Lemont, Illinois 60439, USA*
[4]*Advanced Photon Source, Argonne National Laboratory, Lemont, Illinois 60439, USA*
[5]*St. Petersburg Electrotechnical University LETI, St. Petersburg 197376, Russia*
(Received 5 October 2013; published 18 March 2014)

A tunable energy-chirp compensator was used to remove a correlated energy chirp from the 60-MeV beam at the Brookhaven National Laboratory Accelerator Test Facility. The compensator operates through the interaction of the wakefield of the electron bunch with itself and consists of a planar structure comprised of two alumina bars with copper-plated backs separated by an adjustable beam aperture. By changing the gap size, the correlated energy chirp of the electron bunch was completely removed. Calculations show that this device, properly scaled to account for the electron bunch charge and length, can be used to remove residual correlated energy spread at the end of the linacs used for free-electron lasers. The experimental results are shown to be in good agreement with numerical simulations. Application of this technique can significantly simplify linac design and improve free-electron lasers performance.

DOI: 10.1103/PhysRevLett.112.114801 PACS numbers: 41.60.Bq, 41.75.Ht, 41.85.Ct

Most free electron lasers (FELs) operate using a high electron peak current, which is obtained by compressing the electron bunch in the linac. To achieve compression, the electron bunch is accelerated in the linac off crest and acquires an energy variation that is correlated with the longitudinal coordinate. The linear part of this variation is called the energy chirp (or simply a chirp) and is usually measured in units of MeV/mm. The chirp is defined as positive when the head of the bunch is lower in energy than the tail. When an electron bunch with a positive chirp passes through a longitudinally dispersive magnetic chicane, its head follows a longer path than its tail and the electron bunch compressed when it emerges. At the same time, the chirp grows because the magnitude of the head-to-tail energy variation does not change in the compression process.

This residual chirp is detrimental to the FEL performance and must be removed. Typically, this is done by running the bunch off crest in the linac and also by utilizing the self-wakefield induced by the electron bunch in the accelerating structures (e.g., see [1]). In a normal conducting linac, the wake potential is sufficiently large and there is enough linac length to eliminate the residual chirp. In the superconducting linac considered as the most viable candidate for future FELs, the wake potential is weak and cannot totally eliminate the residual energy chirp [2].

An alternative approach suggested in [3] is to use a passive wake-inducing device dubbed as "the wakefield silencer." Similar proposals were also put forward later in [4–6]. A new designation, the "dechirper," was used in [6] and adopted here as a generic name for a passive wakefield-based device whose sole purpose is to modify the energy chirp. Nearly every new FEL project now entertains the idea of using a dechirper to remove the beam chirp [7–10]. With the dechirper, the final bunch compression can be used at the end of the linac allowing acceleration of low peak current bunches with small energy spread, a great advantage for future FELs based on "seeding" techniques. Use of several dechirpers can also help to remove higher-order nonlinearities, a methodology that we defer for future studies.

The experimental verification of the idea of the dechirper was first obtained in [5] where a set of dielectric-lined cylindrical waveguides with different apertures was used to produce wake potentials with variable strengths. Although, the use of a variable aperture gives a reasonable flexibility in adjusting the dechirper strength, a continuously tunable dechirper is preferred. Naturally, a tunable dechirper will allow using customizable electron bunch parameters at each individual undulator line in an undulator "farm" serviced by a single high repetition rate linac. In this Letter we describe such a device and present experimental results obtained by using it.

Figure 1 shows a photo and a schematic of a *tunable* dechirper. Each vertical copper wall holds a 10-cm-long, 12-mm-high, 6.35-mm-wide alumina bar with dielectric constant $\varepsilon = 9.8$. The gap between the bars is regulated by a stepping motor (not shown in the photo).

While propagating through the dechirper, the electrons emit Cherenkov radiation producing the wakefields affecting trailing electrons. The impact of these fields is traditionally described using the wakefield potential $W(x, y, s)$

 © 2014 American Physical Society

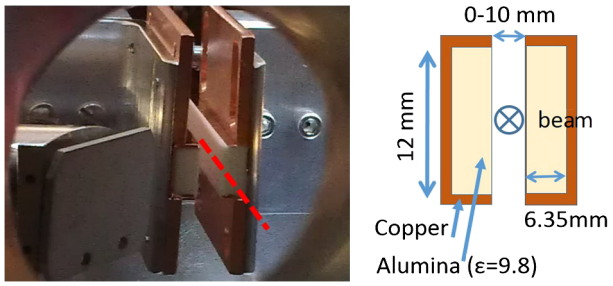

FIG. 1 (color online). A planar tunable dechirper. (Left) The dashed red line in the center of the photo shows the electron beam trajectory. (Right) A schematic of the dechirper.

that defines the energy loss of a particle with the (x, y) transverse coordinates and within a longitudinal position s with respect to the center of a bunch. Once the wakefield potential $G(x, y, x', y', s - s')$ of a point charge at a location (x', y', s') is known, then the wakefield potential of an arbitrary charge $q(x', y', s')$ can be found from a convolution integral:

$$W(x,y,s) = \frac{1}{Q}\oint \int_{-\infty}^{s} G(x,y,x',y',s-s')q(x',y',s')dx'dy'ds' \tag{1}$$

where Q is the total charge of the bunch. Following [11], $G(x, y, x', y', s - s')$ can be found performing summation of all modes synchronous with the electron bunch:

$$G(x,y,x',y',s-s') = \sum_{i=1}^{N} A_i(x',y')E_i(x,y)\cos[k_i(s-s')], \tag{2}$$

where each function $A_i(x', y')$ defines efficiency of excitation of the ith longitudinal mode with the wave vector k_i and transverse field distribution $E_i(x, y)$ by the a point charge at a location (x', y'). These functions can be obtained following the methodology described in [11].

The wake potential amplitude is proportional to $\eta Q/a^2$, where η is the geometric form factor, Q is the charge, and a is the characteristic size of the aperture. Hence, tuning the transverse size of the aperture allows corresponding adjustment of the strength of the chirp corrector [12].

Removing a linear chirp requires the decelerating wake potential to be linear over the entire bunch length. In practice, the extent over which the wake potential remains linear depends on the charge distribution in the electron bunch and the thickness of the dielectric layer. In Fig. 2(a), we present plots of the wake potentials produced by a 300-pC electron bunch with a flattop current distribution considered as the best option in many FEL projects [i.e., see Next Generation Light Source [13]]. Calculations were carried out for the dechirper shown in Fig. 1 using the method described above and in Ref. [14]. A specific charge distribution with a 150-μm-long flattop and smooth edges was used. Since the impact of the dechirper linearly scales with the length of the device and the charge of the electron bunch, it is convenient to characterize the dechirper strength in units of MeV/mm/m/nC. Using a linear fit to the wake potential as illustrated in Fig. 2(b), we computed the dechirper strengths $S_D = 40.7$, 78.5, and 197 MeV/mm/m/nC corresponding to gaps = 2.8, 1.9, and 1 mm, respectively.

For a successful single stage dechirper (whose short-range wake potential has a nearly linear profile over most of the length of the electron bunch), the low-frequency modes in the wake potential with wavelengths longer than the bunch length need to dominate the higher-frequency modes. This can be accomplished by selecting the thickness of the dielectric layer and by adjusting the dechirper gap. The tradeoff between these options is shown in Fig. 3. Figure 3(a) shows the calculated short-range wake potential produced by a 300-pC electron bunch with a 150-μm-long

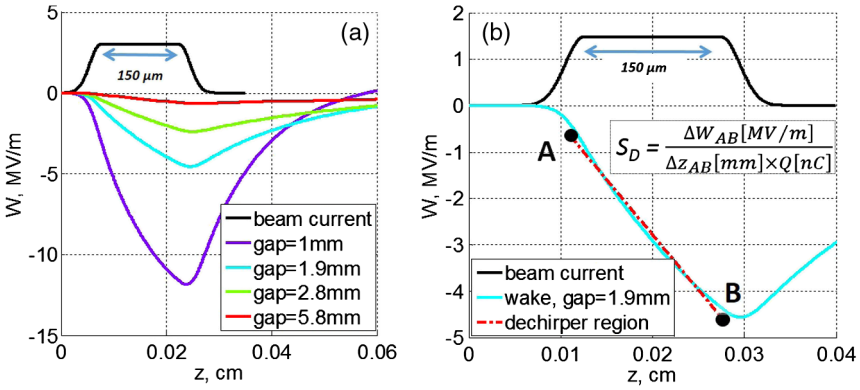

FIG. 2 (color online). (a) Short-range wake potential calculated for four values of the dechirper gaps indicated on the plot. (b) Illustration of the definition of the dechirper strength using the linear fit of the wake potential between points A and B (the case with 1.9-mm dechirper gap was used). The black curve shows the profile of the electron charge distribution.

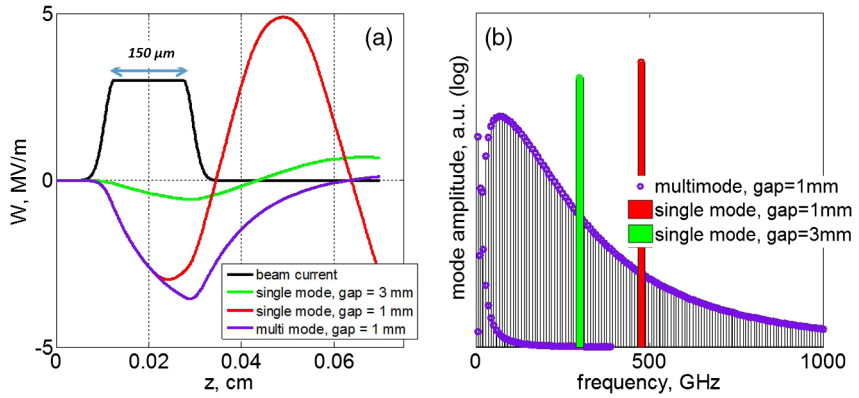

FIG. 3 (color online). (a) Calculated short-range wake potential produced by the electron bunch with a 150-μm-flattop (black curve) in a dechirper with a 6.35-mm dielectric layer (red curve) and a dechirper with a 20-μm dielectric layer (purple and green curves). The dechirper gap is indicated on the plot for each case. (b) Spectrum of the wake potentials. The colors of the spectral lines in this panel match the colors of the wakefield curves in panel (a).

flattop segment in a 1-mm gap, 10-cm-long dechirper with a 6.35-mm-thick alumina layer, and in a similar dechirper with a 20-μm-thick alumina layer.

While a thick-layer dielectric-loaded waveguide hosts many modes, as seen in Fig. 3(b), a thin-layer structure effectively has only one excited mode. In the case of a thick dielectric layer (multimode structure), a quasilinear wake potential (shown by the purple curve) extends over the length of the flattop segment. In the case of an ultrathin dielectric layer (single mode), the wake potential (shown with the red curve) begins to significantly deviate from a linear function at an approximate distance of 100 μm, comparable to the wavelength of the mode shown in Fig. 3(b), where the calculated spectrum of the wake potentials is given. One can also see in Fig. 3(b) that increasing the gap of the single mode dechirper from 1 to 3 mm shifts the mode frequency from 477 GHz to approximately 299 GHz and extends the quasilinear chirp of the wake potential to 150 μm (as shown by the green curve). However, this also leads to a reduction in the dechirper strength from $S_D = 197$ MeV/mm/m/nC to $S_D = 32$ MeV/mm/m/nC. If the thickness of the dielectric layer were to be increased (to about 50 μm) to shift the frequency of the excited mode down to 300 GHz and extend the quasilinear region, the new structure could be used for chirp correction. For ease of handling and construction, we chose to use a thick dielectric loading based on readily available stock ceramic pieces, 6.35 mm thick.

One conclusion that can be drawn from the above analysis is that it is possible to use a combination of two or more dechirpers with different thicknesses of the dielectric layers and different gaps to remove a nonlinear energy chirp, by designing each stage to remove a separate Fourier component of the wake potential. Having a tunable dechirper for this task seems to be even more important since the exact type of nonlinearity in the chirp may not be known initially or can change depending on specific electron beam and linac parameters.

The experiment using a tunable dechirper was performed at the Accelerator Test Facility at Brookhaven National Laboratory [15]. Figure 4 shows the general experimental layout. For this experiment, the electron bunch was accelerated off crest in the linac (to introduce a positive 0.33-MeV/mm energy chirp) to 60 MeV and sent through a "dogleg" type magnetic achromat with two identical dipole magnets at the beginning and two similar dipole magnets with the opposite polarity at the end and the quadruple magnets in between (not shown in Fig. 4). A beam collimator mask is placed at the high dispersion point between the

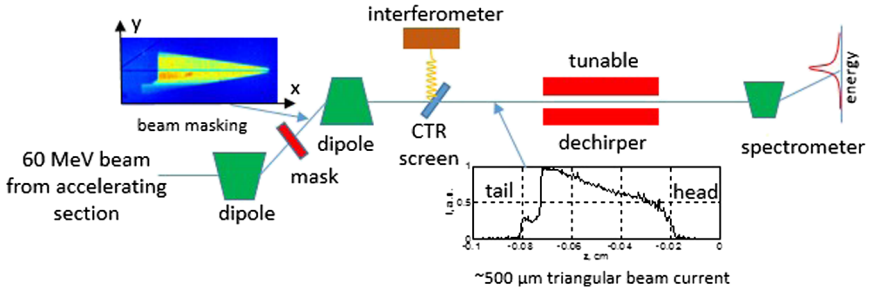

FIG. 4 (color online). Schematic of the experimental setup.

dipoles where the beam transverse size is dominated by the correlated energy spread induced in the linac. Therefore, the transverse pattern introduced by the mask appears in the longitudinal charge density distribution after the achromat. Therefore, the image of the beam taken directly after the mask and shown in Fig. 4 represents the longitudinal beam distribution shown in Fig. 6(a) [16]. To calibrate this correspondence two beamlets were created by the mask. The actual distance between these beamlets appearing in the longitudinal direction after the dogleg was measured by the interferometer equipped with a helium-cooled bolometer [16] that received the CTR signal emitted by the beamlets passing through a thin foil. From these measurements the distance between beamlets was determined and the phosphor screen image after the mask was calibrated.

The triangular collimator mask was used to yield a peak current distribution with a quasi-triangular profile, as shown in Fig. 4. The length of the base of the triangle was approximately 500 μm, and the total charge of the electron bunch after the mask was 54 ± 1.6 pC. Selection of the triangular profile for the peak current in the experiment helped maintain a linear chirp over the long electron bunch necessary to obtain a reasonably large energy chirp in the linac. We were not able to generate a short bunch with a large chirp using the ATF linac. The electron beam energy chirp was then manipulated by passing the electron bunch through a dechirper, as shown in Fig. 1. After that, the electron bunch was sent into a spectrometer where its energy spread was measured. In general, when beam passes the structure off-axis it produces a transverse wake which can distort its phase space. Collecting the data, we kept the electron bunch centered in the tunable dechirper with better than 10 μm accuracy in order to keep the degradation of the projected emittance by transverse wakefields below ~10% (an estimate obtained for the 1 mm gap following [6]). We were not able to resolve in the experiment the impact of the higher order transverse wakefields.

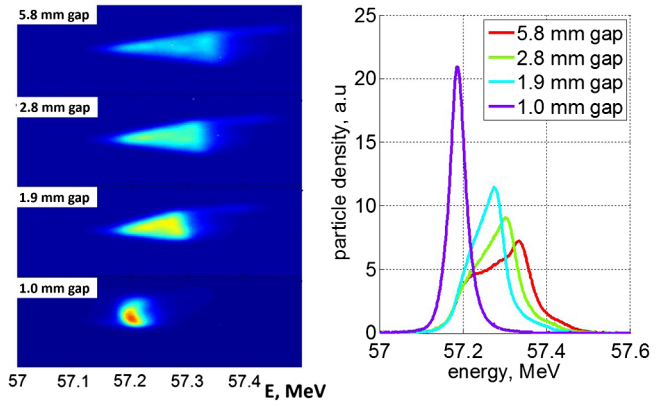

FIG. 5 (color online). (a) Phosphor screen images of the beam passing through the dechirper with gap sizes of 5.8, 2.8, 1.9, and 1 mm. (b) The electron energy distribution derived from the images in the left panel.

Figure 5 shows the raw experimental data and the processed data. In the left panel one can see images of the electron bunch on a phosphor screen at the end of the spectrometer where the horizontal coordinate corresponds to the electron energy, and the vertical coordinate the electron vertical offset. Beam shaping by means of a mask in the dispersive section described above [16] requires a beam with a correlated energy chirp and because of this correlation a quasi-triangular longitudinal profile of the beam [Figs. 4(a), 6(a)] appears on the spectrometer image [Fig. 5(a)]. In the right panel one can see the energy distribution of the electrons. Before measurements, the spectrometer was calibrated using the bending magnet, and an energy resolution of 30 keV was found. The scale on the horizontal axes in Fig. 5 shows the actual electron energy.

The initial correlated energy spread with the dechirper gap open to 5.8 mm was measured to be 165 keV. Thus, assuming a 500 μm bunch length, we calculated that the energy chirp was 0.33 MeV/mm. The decrease in the

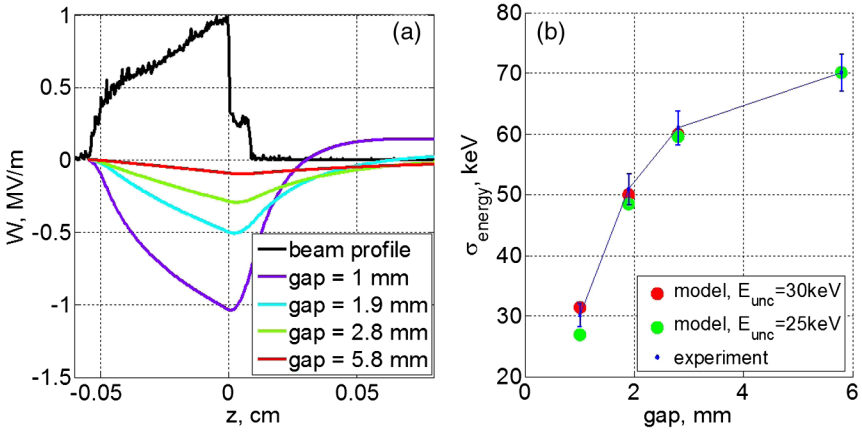

FIG. 6 (color online). (a) Wake potential calculated using the measured electron peak current distribution (black curve) and 300-pC bunch charge for various dechirper gap values indicated on the plot. (b) The rms electron bunch energy spread as a function of the dechirper gap. Experimental results are shown with blue squares; calculations are shown with circles.

correlated energy spread was observed as the dechirper gap was gradually closed from 5.8 to 1 mm. At a gap size of 1 mm, the correlated energy spread was found to be at a minimum. Since the energy spread was compensated in the 10-cm-long dechirper and the total bunch charge was 54 ± 1.6 pC, the dechirper strength was found to be $S_D = 61 \pm 6$ MeV/mm/m/nC where the error includes contributions from the energy calibration, charge fluctuations, and bunch length measurement.

Finally, we used the measured electron peak current distribution and the electron bunch charge and calculated the wake potential produced by the bunch in the dechirper for the dechirper gaps used in the experiment. The result is plotted in Fig. 6(a). For the measured beam profile we assigned the energy distribution composed of the correlated and uncorrelated energy spread. Because of the limited spectrometer resolution, we could not measure the uncorrelated spread directly. For our model we compared two cases of uncorrelated energy spread: −25 and 30 keV. We picked the energy chirp to match the energy spread of the case when the dechirper is fully open. Further, we calculated the rms energy spread in the electron bunch after the dechirper and compared it with measurements. The errors for the energy measurement were determined by the spectrometer calibration. The comparison is shown in Fig. 6(b) where one can see that results agree very well within the error bars. This means that we can use a linear model to predict the dechirper performance for a given beam.

To summarize, a planar tunable dechirper with a strength up to $S_D = 61$ MeV/mm/m/nC was successfully demonstrated in the experiment conducted at the Brookhaven National Laboratory Accelerator Test Facility. By closing the dechirper gap from 5.8 to 1.0 mm, the initial electron bunch energy chirp of 0.33 MeV/mm was gradually reduced to 0. The residual energy distribution with rms value of 30 keV corresponded to the estimated uncorrelated beam energy spread. This result gives a strong justification and a proof of principle for a tunable dechirper that, when properly scaled, can be used to remove the residual correlated energy spread at the end of the linacs used for free-electron lasers (FEL). Potentially, this device can significantly simplify a linac design and improve the performance of FELs. In this Letter we described a dechirper intended to remove the linear energy chirp. In principle, a more complicated dechirper or a combination of several similar dechirpers with various thicknesses of dielectric layers could also be used to remove nonlinear time-dependent energy correlations in the electron bunch.

Euclid Techlabs LLC acknowledges support from the DOE SBIR program Grant No. DE-SC0006299. Work at Argonne National Laboratory is supported by the U.S. Department of Energy, Office of Science, under Contract No. DE-AC02-06CH11357. Work at Brookhaven National Laboratory is supported by the U.S. Department of Energy, Office of Science, under Contract No. DE-AC02-98CH10886.

Note added.—After this manuscript was submitted, we learned about another successful dechirping experiment performed by the collaboration from LBNL, SLAC, and POSTECH cited in Refs. [7,17].

[1] M. Dohlus, T. Limberg, and P. Emma, in *Beam Dynamics Newsletter, N38*, edited by I. S. Ko (2005), http://www-bd.fnal.gov/icfabd/Newsletter38.pdf.
[2] R. Bartolini *et al.*, in *Proceedings of the Particle Accelerator Conference (PAC'09), Vancouver, Canada, 2009* (IEEE, New York, 2009), pp. 1226–1228.
[3] M. Rosing and J. Simpson, ANL Report No. WF-144, 1990.
[4] P. Craievich, Phys. Rev. ST Accel. Beams **13**, 034401 (2010).
[5] S. Antipov, C. Jing, M. Fedurin, W. Gai, A. Kanareykin, K. Kusche, P. Schoessow, V. Yakimenko, and A. Zholents, Phys. Rev. Lett. **108**, 144801 (2012).
[6] K. L. F. Bane and G. Stupakov, Nucl. Instrum. Methods Phys. Res., Sect. A **690**, 106 (2012).
[7] H. S. Kang, Proceedings of FEL'2013 (2013), http://accelconf.web.cern.ch/AccelConf/fel2013/talks/moicno02_talk.pdf.
[8] K. L. F. Bane and G. Stupakov, SLAC Report No. SLAC-PUB-15852, 2013.
[9] K. Bane, P. Emma, Z. Huang, R. Iverson, T. Raubenheimer, G. Stupakov, and L. Wang, SLAC Report No. SLAC-PUB-15853, 2013.
[10] S. Bettoni, P. Craievich, M. Pedrozzi, and S. Reiche, *Proceedings of International Free Electron Laser Conference (FEL'13), New York, NY, 2013* (2013), pp. 214–216, https://accelconf.web.cern.ch/AccelConf/FEL2013/papers/tupso04.pdf.
[11] L. Xiao, W. Gai, and X. Sun, Phys. Rev. E **65**, 016505 (2001).
[12] S. Antipov *et al.*, *Proceedings of the International Particle Accelerator Conference (IPAC'12), New Orleans, LA, 2012* (IEEE, New York, 2012), pp. 598–600.
[13] J. N. Corlett *et al.*, *Proceedings of the International Particle Accelerator Conference (IPAC'12), New Orleans, LA, 2012* (IEEE, New York, 2012), pp. 1762–1764.
[14] S. S. Baturin, I. L. Sheinman, A. M. Altmark, and A. D. Kanareykin, Phys. Rev. ST Accel. Beams **16**, 051302 (2013).
[15] V. Yakimenko, AIP Conf. Proc. **737**, 677 (2004).
[16] P. Muggli, V. Yakimenko, M. Babzien, E. Kallos, and K. P. Kusche, Phys. Rev. Lett. **101**, 054801 (2008).
[17] P. Emma, M. Venturini, K. L. F. Bane, G. Stupakov, H.-S. Kang, M. S. Chae, J. Hong, C.-K. Min, H. Yang, T. Ha, W. W. Lee, C. D. Park, S. J. Park, and I. S. Ko, Phys. Rev. Lett. **112**, 034801 (2014).